

Characterization of abalone *Haliotis tuberculata*–*Vibrio harveyi* interactions in gill primary cultures

Delphine Pichon^{1,*}, Benoit Cudennec^{2,5}, Sylvain Huchette³, Chakib Djediat⁴, Tristan Renault⁵,
Christine Paillard⁶, Stéphanie Auzoux-Bordenave^{1,7}

¹ Station de Biologie Marine, Muséum National d'Histoire Naturelle, DMPA, UMR BOREA 7208 CNRS/MNHN/IRD/UPMC, 29900, Concarneau, France

² Laboratoire ProBioGEM, Université Lille 1, 59655, Villeneuve-d'Ascq, France

³ France-Haliotis, 29880, Plouguerneau, France

⁴ Plateforme d'Imagerie et de Microscopie Electronique (PIME), Muséum National d'Histoire Naturelle, 12 rue Buffon, 75005, Paris, France

⁵ Unité Santé, Génétique et Microbiologie des Mollusques—Laboratoire de Génétique et Pathologie des Mollusques Marins, Ifremer, 17390, La Tremblade, France

⁶ UMR6539 CNRS/UBO/Ifremer/IRD, LEMAR Université de Bretagne Occidentale, 29280, Plouzané, France

⁷ Université Pierre et Marie Curie Paris VI, 4 Place Jussieu, 75005, Paris, France

*: Corresponding author : Delphine Pichon, email address : pichon@mnhn.fr

Abstract:

The decline of European abalone *Haliotis tuberculata* populations has been associated with various pathogens including bacteria of the genus *Vibrio*. Following the summer mortality outbreaks reported in France between 1998 and 2000, *Vibrio harveyi* strains were isolated from moribund abalones, allowing in vivo and in vitro studies on the interactions between abalone *H. tuberculata* and *V. harveyi*. This work reports the development of primary cell cultures from abalone gill tissue, a target tissue for bacterial colonisation, and their use for in vitro study of host cell—*V. harveyi* interactions. Gill cells originated from four-day-old explant primary cultures were successfully sub-cultured in multi-well plates and maintained in vitro for up to 24 days. Cytological parameters, cell morphology and viability were monitored over time using flow cytometry analysis and semi-quantitative assay (XTT). Then, gill cell cultures were used to investigate in vitro the interactions with *V. harveyi*. The effects of two bacterial strains were evaluated on gill cells: a pathogenic bacterial strain ORM4 which is responsible for abalone mortalities and LMG7890 which is a non-pathogenic strain. Cellular responses of gill cells exposed to increasing concentrations of bacteria were evaluated by measuring mitochondrial activity (XTT assay) and phenoloxidase activity, an enzyme which is strongly involved in immune response. The ability of gill cells to phagocyte GFP-tagged *V. harveyi* was evaluated by flow cytometry and gill cells-*V. harveyi* interactions were characterized using fluorescence microscopy and transmission electron microscopy. During phagocytosis process we evidenced that *V. harveyi* bacteria induced significant changes in gill cells metabolism and immune response. Together, the results showed that primary cell cultures from abalone gills are suitable for in vitro study of host-pathogen interactions, providing complementary assays to in vivo experiments.

Keywords: *Haliotis tuberculata* ; *Vibrio harveyi* ; Gill cell culture ; Pathogenicity ; Phenoloxidase ; Phagocytosis

1. Introduction

Diseases affecting cultured molluscs are caused by protozoans, fungi, bacteria or viruses, leading to severe damages at any stage of production from larvae to adults (Paillard et al. [2004](#)). Bacterial diseases like Brown Ring disease (BRD) and Juvenile oyster disease (JOD) caused high mortalities in hatcheries and were commonly described in larval and adult bivalves (Lauckner [1983](#); Paillard et al. [2004](#); Paillard and Maes [1989](#); Boettcher et al. [1999](#), [2000](#)). Summer mortalities caused by *Vibrio* bacterial strains have recently been described in various cultured mollusc as the Pacific oyster *Crassostrea gigas* (Le Roux et al. [2002](#); Saulnier et al. [2010](#)) and the European abalone *Haliotis tuberculata* (Nicolas et al. [2002](#)). European abalone stocks are currently threatened by several pathogens causing severe mass mortalities in wild or farmed populations, among them *Xenohaliotis californiensis*, *Haplosporidium* sp. and *Vibrio harveyi* (Nicolas et al. [2002](#); Azevedo et al. [2006](#); Balseiro et al. [2006](#); Huchette and Clavier [2004](#)).

Vibrio harveyi (Syn. *V. carchariae*) is a marine bacterium common in the ocean (Gauger and Gomez-Chiarri [2002](#)), and known to be pathogenic in a large range of vertebrates and invertebrates including molluscs (Austin and Zhang [2006](#)). Abalone diseases due to the pathogen *V. harveyi* have been already described for *Haliotis diversicolor* (Nishimori et al. [1998](#)), for *Haliotis laevis* (Handlinger et al. [2005](#); Vakalia and Benkendorff [2005](#); Dang et al. [2011a](#)) and for *H. tuberculata* (Nicolas et al. [2002](#)), in tropical or temperate seawater, causing septicaemia. Since 1998, summer mass mortality outbreaks of the European abalone *H. tuberculata* reported along the north coast of Brittany (France) have been associated with *Vibrio* bacteria (Nicolas et al. [2002](#)). Bacterial strains were isolated from both farmed and wild abalones, allowing in vivo and in vitro studies on the interactions between abalone *H. tuberculata* and *V. harveyi* (Nicolas et al. [2002](#); Travers et al. [2008b](#), [2009](#)). *Vibrio harveyi* is an opportunistic bacterium becoming pathogenic if immunity is compromised due to summer heat stress, poor water quality or reproduction period (Cheng et al. [2004a](#), [b](#); Vakalia and Benkendorff [2005](#); Hooper et al. [2007](#); Travers et al. [2008b](#); Mottin et al. [2010](#); Dang et al. [2011a](#), [b](#); Latire et al. [2012](#)). Considering the development of aquaculture in Europe (Huchette and Clavier [2004](#)), the evolution of

64 reliable diagnostic tools is of major importance for the control and prevention of bacterial diseases (Paillard et al. 2004).
65 Cell cultures provide alternative and controlled experimental models for basic research as well as with various
66 applications in pathology, ecotoxicology and natural compounds production (Rinkevich 1999, 2011, Auzoux-Bordenave
67 and Domart-Coulon 2010). Although there is currently no cell lineage in marine invertebrates, primary cell cultures
68 provide suitable tools for complementary *in vivo* studies. Invertebrate immune defence is mainly mediated by
69 circulating hemocytes (Smith 1991), including phagocytosis, encapsulation, production of antimicrobial compounds as
70 well as the phenoloxidase cascade that is an important reaction of melanisation involved in immunity (Cheng 1981,
71 Bachère et al. 1995, Hooper et al. 2007, Travers et al. 2008c).

72 Antibacterial activity of abalone hemolymph has been demonstrated against *Vibrio* using *in vitro* assays (Vakalia and
73 Benkendorff 2005, Travers et al. 2009, Dang et al. 2011a, 2011b) such as phagocytosis, ROS activity or phenoloxidase
74 activity, and secretion of antibacterial peptides or lipophilic antibacterial compounds. The immune response of abalone
75 hemocytes has been previously shown to change according to the pathogenicity of bacterial strains (Travers et al. 2009).
76 Thus pathogen strains would be able to proliferate in contact with hemolymph avoiding phagocytosis and preventing
77 immune response. Moreover, only few host responses were investigated based on cell morphology or using cultured
78 hemocytes (Nicolas et al. 2002, Travers et al. 2008c). While primary culture of hemocytes have been previously used
79 for studying host-pathogen interactions at a cellular level (Boulo et al. 1991, Ford and Ashton-Alcox 1993) there are
80 only few assays using other target tissues such as mantle, digestive gland or gills (Dang et al. 2011b, Faucet et al.,
81 2003).

82 The present work aimed at studying abalone *Haliotis tuberculata-Vibrio harveyi* interactions in gill primary cultures.
83 Explant cultures were developed from the gills, a target tissue for bacterial infection, and subcultured to perform *in vitro*
84 pathogenicity assays. The characterization of cell morphology, viability and the physiological status of the cells were
85 monitored over culture time using flow cytometry and semi-automated assay (XTT). Gill cell cultures were used to
86 investigate *in vitro* the mode of action of two bacterial strains of *V. harveyi*. The responses of gill cells to *V. harveyi*
87 bacteria, including phagocytosis, were evaluated by using a combination of semi-quantitative enzymatic *in vitro* assays
88 (XTT, phenoloxidase), flow cytometry analyses, as well as fluorescence and transmission electron microscopy analysis.

89

90 **Material and methods**

91 *Animals*

92 European adult abalone (*Haliotis tuberculata*), 40 to 60 mm shell length, were collected from the France-Haliotis farm
93 (Plouguerneau, Brittany). The animals were maintained at the laboratory in an 80 L tank supplied with aerated natural
94 seawater. Abalones were fed once a week with red algae *Palmaria palmata*. Two days before experiments, abalones
95 were starved and seawater was UV treated to prevent contamination.

96

97 *Bacterial strains*

98 Two *Vibrio harveyi* strains were used for *in vitro* pathogenicity assays: a virulent strain ORM4 isolated from moribund
99 abalone in 1998 (Nicolas et al. 2002) and a non pathogenic strain LMG7890 (former *V. carchariae* type strain) isolated
100 from dead brown shark *Carcharinus plumbeus* (Colwell 1982). For microscopic observations and bacterial phagocytosis
101 assays, GFP-tagged *V. harveyi* strains were used (Travers et al. 2008a).

102 The two bacterial strains were cultured on Luria Bertani Agar (Sigma, St. Louis, MO, USA) supplemented in salinity
103 (to 20 g.L⁻¹) and incubated at 28°C for 24h. For *in vitro* contact, bacterial strains were washed in sterilized seawater.
104 Bacterial concentrations were determined by optical density measurements at 490 nm. For all tests controls consisted of
105 cells without bacteria, and cells with heat inactivated bacteria.

106

107 *Gill cell primary culture*

108 Primary cultures were performed according to the explant method previously developed for mollusc mantle culture
109 (Auzoux-Bordenave et al. 2007) and recently adapted to the gills by Gaume et al. (2012). The gills were aseptically
110 dissected and placed for 2 days in an antiseptic solution (= natural filtered sea water containing 200 U/mL penicillin–
111 200 Ig/mL streptomycin (Sigma), 250 Ig/mL gentamycin (Sigma) and 2 Ig/mL amphotericin B (Sigma)). Tissues were
112 then minced into 2-3 mm³ explants which were placed to adhere onto the bottom of plastic 6-well plates. After 30 min
113 of adhesion, explants were covered with 1 mL modified Leibovitz (Sigma) L-15 medium adjusted to 1100 mosm.L⁻¹ by
114 addition of mineral salts and supplemented with 100 U.mL⁻¹ penicillin-streptomycin (Sigma), 200 µg.mL⁻¹ gentamycin
115 (Sigma) and 1 µg.mL⁻¹ amphotericin B (Sigma) to limit external contamination. The pH was adjusted to 7.4. Explant
116 primary cell cultures were incubated at 18°C in a humidified incubator and observed daily with an inverted phase
117 contrast microscope (Telaval 3, Jena).

118 After 4-5 days of primary culture, a large quantity of gill cells was generated from the explants and the cells were
119 collected. Cell suspension was strained on a 70µm mesh filter (Cell strainer, VWR Internat.), resuspended in modified
120 L-15 medium and assessed for cell density using a hemocytometer. Cells were subcultured in multi-well microplates to
121 perform *in vitro* assays. For optimal cellular response, cell density was adjusted to 500,000 cells/well in 24-well
122 microplates (Dutscher) and 150,000 cells/well in 96-well microplates (Dutscher).

123

124 *Cell population distribution*

125 Analyses were performed using FACS Calibur flow cytometer (Becton Dickinson) equipped with a 488nm laser. 1000
126 events were counted for each sample. Results are expressed as cell cytogram indicating the size (FSC value), the
127 complexity (SSC value), and the level of fluorescence. Cells were incubated for 30 min with SYBR Green fluorescent

128 dye (Molecular Probes) at 10^{-3} dilution of the commercial stock solution. Gill cells were gated to estimate the
129 population distribution in terms of forward scattering (FSC, size) and side scattering (SSC, granularity and volume).

130

131 *Phagocytosis assay*

132 Phagocytosis assays were performed by flow cytometry according to the protocol for hemocytes adapted from Allam et
133 al. (2002). After four days explant culture, gill cells were collected and diluted in L-15 culture medium. Phagocytosis
134 index was defined by the percentage of cells ingesting three or more fluorescent beads, and was measured by flow
135 cytometry. 10 μ l of bead solution (Fluorospher, Invitrogen) was added to 200 μ l of cell suspension (700 beads per cells),
136 and were incubated for 1 hour at room temperature in the dark. Flow cytometry analysis was performed as described
137 previously. Results are expressed as cell cytogram indicating the size (FSC value), the complexity (SSC value), and the
138 level of fluorescence.

139 To measure the ability of gill cells to phagocyte the two *Vibrio harveyi* strains, the same protocol was used. GFP-tagged
140 bacterial strains were added to the culture and incubated at room temperature in the dark for 1 hour, 2 hours and 20
141 hours. Fluorescence was measured by flow cytometry. Data obtained were the means \pm SE of three values expressed as
142 percentage of fluorescence, and statistical analysis was performed using a two-sample *t*-test, with significance at
143 $P < 0.005$.

144

145 *XTT Reduction Assay*

146 Cellular activity was measured by the XTT assay (Roche Laboratories, Meylan, France) based on the reduction of a
147 tetrazolium salt (XTT-sodium 3'-[1-(phenylaminocarbonyl)-3,4-tetrazolium]-bis (4-methoxy-6-nitro) benzene sulfonic
148 acid hydrate) into yellow formazan salt by active mitochondria (Mosmann 1983). The XTT assay, previously adapted to
149 mollusc cells, provides a global evaluation of the number of viable cells through the measurement of their mitochondrial
150 activity (Domart-Coulon et al. 2000). Assays were performed in 96-well microplates. For this, 50 μ L of a mixture of
151 XTT/PMS (N-methyl dibenzopyrazine methyl sulfate) was added to 100 μ L of cells/well. Plates were incubated for 20h
152 at 18°C, and the intensity of the coloration was measured by spectrophotometry at 490 nm with a 655 nm reference
153 wave-length (BioTek plate reader). For *in vitro* assays, bacterial concentration was adjusted in seawater, and 50 μ L of
154 this mixture were added to the cell culture for 1, 5 and 20 hours. After the required incubation time, XTT assay was
155 performed as described before.

156 Data obtained were the means \pm SE of six values expressed as optical density (OD). The effects of bacteria on cell
157 viability were expressed as percentage of the control (cells without contaminant). Statistical analysis was performed
158 using a two-sample *t*-test, with significance at $P < 0.005$.

159

160 *Phenoloxidase Activity*

161 Since the phenoloxidase enzyme is strongly involved in immune response, the assessment of its activity is frequently
162 used to evaluate the cell response to external contaminants (Bachère et al. 1995, Cerenius et al. 2008, Hellio et al 2007).
163 Phenoloxidase activity assays were performed in 96-well microplates. 50 µL of TrisHCl buffer (0.2M, pH 8.0) and 10
164 µl L-DOPA (L-3,4-dihydroxyphenyl-alanine, 20 mM, Sigma) were added to supernatant of 200000 cells. The microplate
165 was mixed gently for 10s prior measurement. Detection of phenoloxidase activity was carried out by the measurement
166 of L-3-4-dihydroxyphenylalanine (L-DOPA) transformation in dopachromes. The colorimetric reaction was measured
167 in triplicate at room temperature every 10 min for 100 min at 492 nm, and expressed as changes in optical density per
168 mg of protein. Controls consisted of TrisHCl and L-DOPA without cells or bacteria, and were performed in parallel
169 assays. Protein amount in each test, cellular extract and controls, were determined by the Bradford method (Bradford
170 1976), with serum albumin as a standard. Data obtained were the means \pm SE of six values expressed as OD. The impact
171 of bacteria on the phenoloxidase activity was expressed as percentage of control (cells without contaminant). Statistical
172 analysis was performed using a two-sample *t*-test, with a significant at $P < 0.005$.

173

174 *Fluorescence microscopy*

175 Gill cells, four days old subcultured, were incubated in the presence of the two GFP-tagged bacterial strains for one or
176 two hours and immediately observed with a direct fluorescence microscope (Olympus).

177

178 *Transmission electron microscopy*

179 Four days old subcultured gill cells were incubated for 2 h with *V. harveyi* bacterial strains. For ultrastructural analysis,
180 gill cells were fixed with 2% glutaraldehyde in 0.1 M Sørensen phosphate buffer containing 0.6 M sucrose at pH 7.4.
181 Cell samples were post-fixed in 2% OsO₄ in Sørensen phosphate buffer (0.18M = 5.33g/L NaH₂PO₄·2H₂O (Sigma)
182 and 20,7g/L Na₂HPO₄ (Sigma) in distilled water (pH 7.4)) for 1 h at room temperature, then rinsed three times in
183 Sørensen buffer, dehydrated in ethanol and embedded in Spurr's resin (Electron Microscopy Sciences, Aygnèsvives,
184 France). Ultra-thin sections (about 50 nm) were cut on an Ultracut Microtome (Ultramicrotomes Reichert-Jung Ultratome
185 E) with a diatome Ultra 45° diamond, and mounted on formavar-coated Cu-grids (Electron Microscopy Sciences),
186 stained with uranyl acetate 2% in 50% ethanol and observed at 75kV with Hitachi H-7100 transmission electron
187 microscope (Tokyo, Japan) equipped with a digital CCD Hamamatsu Camera.

188

189 **Results**

190 *Cell culture from abalone gills*

191 After one day of primary culture, 80% of the explants adhered to the flask bottom and gill cells started to migrate out of

192 the explant (Fig 1a). During the first three days of culture, a large quantity of gill cells was generated from the explants
193 and the cells were spread out onto the bottom of the flask. Gill cell population consisted of a majority of rounded
194 epithelial cells (Fig 1a), glandular cells (Fig 1b) and hemocytes (Fig 1c). The ciliary activity of epithelial cells within
195 the gill filaments demonstrated the vitality of explant primary cultures, according to previous observations from Gaume
196 et al (2012). Typical hemocyte morphological cell types were recognized *in vitro* according to previous studies on
197 abalone hemocytes (Auzoux-Bordenave et al. 2007, Travers et al. 2008c): the majority appeared small round and
198 brightly coloured, amoeboid-like, and fibroblastic-like (Fig 1c), most of them adhering strongly to the plastik flask
199 bottom.

200 Ultrastructural observations of cultured cells by TEM allowed the characterization of different cell morphotypes: gill
201 cells consisted of ciliated epithelial cell with cilia, microvilli and numerous mitochondria (Fig 1d) while glandular cells
202 contained mucopolysaccharide vesicles (Fig 1e). Hyalinocytes exhibited a large round nucleus containing electron
203 dense chromatin nucleoli (Fig 1f) and granulocytes contained electron dense granules and exhibited pseudopodia (Fig
204 1g).

205 After 4 to 5 days of primary culture, cells originated from the explants were subcultured in multi-well plates for *in vitro*
206 assays. Subcultured cells exhibited the same morphotypes all along culture time, fibroblastic cells being less numerous
207 compared to the explants culture.

208 Flow cytometry analysis allowed the comparison of freshly isolated gill (Fig. 2a) cells and 3-day-old subcultured gill
209 cells (Fig. 2b). Results showed that freshly dissociated gill cells were mainly composed of small cells with a relative
210 low intracellular complexity. In contrast, subcultures were mainly composed of larger cells harbouring relatively high
211 intracellular complexity, showing the selection of cells following the transfer in subculture.

212 Gill cells were successfully subcultured in multi-well plates and cell viability was evaluated by the XTT assay. A linear
213 relationship between mitochondrial activity and cell number was previously evidenced at any time of cell culture (data
214 not shown). Figure 2c shows the XTT response of subcultured gill cells as a function of cell density, over a 24 days
215 period. The evolution of XTT response (absorbance) showed a slight decrease during the first three days, and an
216 increase in global cell metabolism with cell density overtime. The two concentrations tested, 100,000 and 200,000 cells
217 per well, allowed to adjust the optimal cell density for further *in vitro* assays to 500,000 cells per well in 24 well-plates
218 and to 150,000 cells per well in 96 well-plates respectively.

219

220 *Phagocytosis*

221 After 3-4 days of explant cell cultures, cells were collected, and were brought into contact with fluorescent beads or
222 with pathogenic and non pathogenic *V. harveyi* at different concentrations to evaluate their phagocytosis capacity. Cell
223 population distribution was estimated according to the size (FSC, forward scattering) against complexity (SSC, side

224 scattering) of gill cells stained with SYBR Green after 1 h of contact with fluorescent beads (Fig. 3a). Gill cells which
225 ingested three or more beads displayed a bigger size and a higher complexity than cells which did not ingest beads.
226 Smaller cells did not absorb fluorescent beads. Gill cells were able to phagocytose more than 80% of fluorescent beads as
227 estimated by the phagocytosis index after one hour of incubation (Fig. 3a), and up to 70% of pathogenic and non
228 pathogenic bacterial strains after two hours of contact (Fig 3b, c). For concentrations of 25 or 75 bacteria per cell, the
229 percentage of phagocytosis was significantly increased between one and two hours, with a higher phagocytosis for
230 LMG7890 than for ORM4. When bacteria were placed into saturation relative to gill cell density (100 bacteria per cell)
231 the same phagocytosis ability was observed for the two bacterial strains.

232 Bacterial phagocytosis by gill cells was investigated by TEM and fluorescent microscopy using GFP-tagged bacteria.
233 Control cells did not display any bacteria, either on the outside or the inside of cells. After two hours of contact with
234 both bacterial strains, many bacteria were present around the cells while some of them appeared internalized within the
235 host cells (Fig 4). Some cells appeared to be damaged. Two cell morphotypes were able to phagocytose *Vibrio*: the
236 hemocytes (Fig. 4a) and the epithelial cells (Fig. 4b). Figure 4b shows an encapsulated bacterium in the cytoplasm,
237 residual body after digestion, and condensed mitochondria in an hyperphosphorylation oxydative state. Details of
238 endocytosed bacteria were observed in epithelial cells, with lysosome I digesting bacteria and lysosome II dispensing
239 their enzymatic content (Fig 4c). Fluorescence microscopy observations with GFP-tagged bacteria allowed to localize *V.*
240 *harveyi* bacteria in close proximity to the host epithelial cells and potentially inside the host cell cytoplasm after two
241 hours of contact (Fig 4d). Similar observations were made for the pathogenic ORM4 and the non-pathogenic LMG7890
242 bacterial strains.

243

244 *Effect of V. harveyi on gill cell viability*

245 The effects of *Vibrio harveyi* bacterial strain on gill cell metabolism were evaluated by the XTT assay (Fig 5). Gill cells
246 from 4-day-old subcultures in 96-well plates were exposed to increased concentrations of bacteria (heat inactivated
247 bacteria and 10, 50 and 100 live bacteria per cell), and their XTT responses were measured up to 20 hours, and
248 compared to the metabolism activity of gill cell control. Figure 5 showed that metabolic activity of gill cells decreased
249 in the presence of the two bacterial strains from the first hour, whereas it remained constant for 20 hours for control
250 cells and cells supplemented with dead bacteria. The metabolic activity of gill cell was shown to significantly decrease
251 as a function of bacterial concentration. At a concentration of 100 bacteria per cell XTT response of gill cell decreased
252 to 90% after 20 hours of contact with the pathogen *V. harveyi* ORM4 and 80% with the non pathogen LMG7890. A
253 decrease of 50% of viability was observed at a density of 50 bacteria per cell after 5 hours of contact with ORM4, while
254 this level was reached only after 20 hours with LMG7890, even with a density of 100 bacteria per cell.

255

256 *Effect of V. harveyi on phenoloxidase activity*

257 The immune response of gill cells exposed to bacteria was measured by the phenoloxidase activity, an enzyme strongly
258 involved in the immune response. Phenoloxidase activity of gill cells remained stable for 18 hours without bacterial
259 strains or in presence of dead bacteria, but strongly decreased in a dose dependant manner in presence of the pathogenic
260 and the non pathogenic *V. harveyi*, as shown in Figure 6. For low concentrations (density of 25 bacteria per cell)
261 phenoloxidase activity was slightly reduced during the first five hours, but a significant decrease of phenoloxidase
262 activity was shown after 18 hours of contact. Phenoloxidase activity decreased after 5 hours of contact, with a
263 reduction of 40 to 60% of phenoloxidase activity with concentration of 100 and 200 bacteria per cell respectively, for
264 both strains compared to the control. Similar results were obtained for the pathogenic and the non pathogenic *V. harveyi*.

265

266 **Discussion**

267 In this work, we developed primary cell cultures from *Haliotis tuberculata* gills, which are a target tissue for bacterial
268 infection in marine mollusks. As previously observed in primary cultures of mollusc tissues, the explant method
269 provided a suitable *in vitro* model that contained all the cell types present in the tissue of origin (Kleinschuster et al.
270 1996, Auzoux-Bordenave and Domart-Coulon 2010). Gill cells were successfully sub-cultured for up to 24 days with a
271 persistent metabolic activity as demonstrated by the XTT assay. The decrease of mitochondrial activity over the first
272 four days following subculture initiation may be attributed to the adaptation of cells to *in vitro* conditions. Abalone gill
273 cell primary culture was first performed by Suwattana et al. (2010) on *Haliotis asinina*. These authors reported viable
274 cell cultures for up to 28 days but observed many contaminations due to the initial presence of bacteria in gills before
275 culture. Contaminations by bacteria or fungi remain a real problem in primary cell culture, especially for tissues that are
276 directly exposed to seawater such as the gills and the mantle (Rinkevich 1999, Van der Merwe et al. 2010). In the
277 present work, the addition of antimicrobial components to the culture medium allowed to prevent bacterial and fungal
278 proliferation *in vitro* without damaging gill cell viability.

279 Gill cell cultures exhibited the main morphotypes previously described in mollusc gills and hemocytes *in vivo*, ie.
280 epithelial cells, including glandular cells, and the two categories of hemocytes, i.e. hyalinocytes and granulocytes
281 (Auzoux-Bordenave et al. 2007; Travers et al. 2008c, de Oliveira et al. 2008, Manganaro et al. 2012).

282 Because circulating hemocytes are the first target cells involved in the immune response of marine molluscs, previous
283 studies mainly focused on the interactions between abalone hemocytes and *Vibrio* bacteria. *In vitro* immunity assays
284 based on hemocytes culture allowed to evidence the antibacterial activity of abalone hemocytes exposed to *Vibrio*
285 species (Vakalia and Benkendorff 2005, Dang et al. 2011b, Travers et al. 2009). Significant variations of antibacterial
286 activity of hemocytes were observed depending on environmental conditions such as temperature, quality of seawater,

287 diet, or spawning period (Travers et al. 2008b, Mottin et al. 2010, Dang et al. 2011a, b). Furthermore, immune
288 depression and antibacterial activity were reported in abalones affected by viruses or bacteria in hemolymph but also in
289 the digestive gland (Travers et al. 2009, Dang et al. 2011a).

290 Since the gills are in direct contact with seawater, they represent a target tissue for the entrance and adhesion of
291 bacteria. Moreover the mucus covering the gill filaments may attract or serve as nutrient for various microbes
292 (Rosenberg and Falkovitz 2004, Sharon and Rosenberg 2008). Although the entrance routes of *Vibrio harveyi* bacteria
293 in abalone have not yet been identified, recent studies evidenced that the gills might be directly infected by bacteria
294 (Travers et al. 2008a). In decapod crustacea, the gills have been shown as the main site of bacterial accumulation,
295 suggesting a role of this tissue in the interactions with pathogens (Martin et al. 1993, Alday-Sanz et al. 2002, Burgents
296 et al. 2005).

297 Using cell cultures from gill tissues, the present work aimed at studying the interactions between *Vibrio harveyi* bacteria
298 and gill cells from the abalone (*Haliotis tuberculata*). Flow cytometry analysis combined with microscopic observations
299 evidenced that cultured gill cells were able to phagocytose both pathogenic and non pathogenic *V. harveyi* strains. Vibrios
300 are known to produce compounds that inhibit host hemocyte responses and especially phagocytosis (Labreuche et al.
301 2006, Allam and Ford 2006). Furthermore, *Vibrio* bacteria develop rapidly in the presence of hemocytes and have been
302 shown to interact directly with the hemocytes, preventing immunity and phagocytosis (Travers et al. 2009).
303 Phagocytosis is one of the first lines of defence in molluscs and is mainly performed by hemocytes. Fluorescent
304 microscopy and TEM analysis allowed the identification of internalized bacteria both within hemocytes and epithelial
305 cells. The presence in infected cells of condensed mitochondria in hyperphosphorylation oxydative state demonstrated a
306 high activity induced by bacterial phagocytosis. Furthermore, the identification of lysosomes within the host cells,
307 provided further evidence of bacterial endocytosis *in vitro*. Lysosomes, which are involved in the degradation of the
308 bacterial cell wall, play a crucial role during phagocytosis by secreting hydrolytic enzymes. The use of lysosomes as
309 biomarkers to assess the cytotoxicity of external contaminants has been previously reported on abalone hemocytes
310 (Latire et al. 2012).

311 The gill cell capacity of phagocytosis, measured by flow cytometry was upper than 80%. Only after two hours of
312 contact with the two bacterial strains, gill cells were able to phagocytose 70% of bacteria. Travers et al. (2009) reported an
313 increase in the capacity of hemocytes to phagocytose fluorescent beads in the presence of the non-pathogenic LMG7890
314 bacterial strain. In the same way, we observed that the phagocytic ability of gill cells was higher in the presence of the
315 non-pathogenic strain compared to the pathogenic one. Despite the ability of abalone cells to phagocytose *V. harveyi*, our
316 study evidenced that both viability and immune response of gill cells were directly affected by the two bacterial strains.
317 Although the LMG7890 strain is not pathogenic for abalones *in vivo*, Travers et al. (2009) reported that a direct
318 injection could induce mortalities, but to a lower extent compared to ORM4 strain. In this study, the presence of

319 pathogenic and non-pathogenic bacteria significantly decreased the cell viability in a concentration dependent manner,
320 as measured by metabolic activity assay (XTT). The sharp decrease of cell viability observed in the presence of ORM4
321 bacteria confirmed the virulence of this strain against abalone gill cells. These results differed from those obtained in
322 abalone hemocytes, showing that ORM4 bacterial strain had no significant effect on hemocytes viability, even after 28
323 hours of contact (Travers et al. 2009).

324 In addition to the effects on global cell metabolism, our results demonstrated that the two bacterial *V. harveyi* strains
325 induced a significant decrease of the phenoloxidase activity *in vitro*. Phenoloxidase has been previously detected in the
326 hemolymph of several invertebrates and its activity has been shown to be directly involved in the immune response
327 (Coles and Pipe 1994, Lacoue-Labarthe et al. 2009). Recent studies reported the use of phenoloxidase activity to
328 measure the immune response of abalone hemocytes exposed to various environmental stressors such as temperature,
329 salinity, trace metals and pathogens (Cheng et al. 2004a, b, Travers et al. 2008b, Mottin et al. 2010, Dang et al. 2011b).
330 Since hemocytes are very abundant in gill tissues, the phenoloxidase activity measured *in vitro* may be partly due to the
331 hemocytes. Nevertheless, our results are consistent with previous studies using phenoloxidase activity as a marker to
332 measure the immune response of mollusc to external contaminants (Bachère et al. 1995, Hellio et al. 2007).

333
334 In this study, we evidenced that primary cultures of abalone gills provide suitable models for *in vitro* pathogenicity
335 assays. This work demonstrates for the first time that *V. harveyi* bacteria induced significant alterations on gill cells
336 viability and immune responses, although important phagocytic activity was detected in these target cells. Further
337 studies using other immune indicators such as ROS activity, combined with lysosome quantification in target cells will
338 help specify the mode of action of *Vibrio harveyi* on abalone cells.

339

340 **Acknowledgments**

341 This work was supported by ECC (SUDEVAB N°222156 “Sustainable development of European SMEs engaged in
342 abalone aquaculture”) and the Brittany region (Programme “Ormeaux”, Pôle Mer Bretagne). We thank Marion
343 Cardinaud for the construction of the strain LMG7890-GFP tagged that she kindly provided for *in vitro* biotests on gill
344 cells.

345

346 **List of figures**

347

348 **Figure 1.** Abalone gill cell primary cultures observed under inverted phase contrast microscope (a, b, c) and
349 transmission electron microscopy (d, e, f, g). a: One-day-old gill explant primary gill cells culture from *Haliotis*
350 *tuberculata* showing the outgrowth of cells from an explant in a 6-well plate, b: Three day-old explant primary culture

351 showing cell spreading around the flask bottom. Cell population consisted of rounded epithelial cells (ec), and glandular
352 cells (gc) c: Three day-old explant culture showing hemocytes represented by small hyalinocytes (b) and fibroblastic
353 like cells (f). Transmission electron micrograph of four day-old cell culture, d: epithelial cell, e: mucous cell, f:
354 hyalinocyte, g: granulocyte. ci: cilia, nu: nucleus, mi: microvilli, mu: mucous vesicle, p: pseudopodia of the
355 phagocytosis vesicle in formation, lv: lipofuscin vesicles.

356

357 **Figure 2.** Flow cytometry analysis and mitochondrial activity of gill cells of *Haliotis tuberculata*. Characteristics of cell
358 populations of freshly mechanically dissociated gill (a) and gill cells after 3 days in subculture (b), size (FSC) against
359 internal complexity (SSC) density plot representation, after 30min of incubation with SYBR Green. Evolution of the
360 XTT response of gill cells in subculture (c) at two densities: 100,000 and 200,000 cells/well in 96-well microplates.
361 Data are the means \pm SE of ten values expressed as OD 490nm/655nm.

362

363 **Figure 3.** Phagocytosis by *Haliotis tuberculata* gill cells estimated by flow cytometry. Phagocytosis index was
364 expressed as percentage of gill cells containing three or more beads after one hour of contact (a). Percentage of
365 phagocytosis of gill cells in presence of the pathogenic ORM4 (b) and the non-pathogenic LMG7890 (c) bacterial strain
366 after one and two hours of contact with three densities of bacteria: 25, 75 and 100 bacteria/cell. Data are the means \pm SE
367 of triplicate experiment. Significant differences ($p < 0.05$) from absorbances measured in control cells are indicated by an
368 asterisk.

369

370 **Figure 4.** Phagocytosis by *Haliotis tuberculata* gill cells after two hours of contact observed by TEM and fluorescent
371 microscopy. a: internalization of ORM4 bacteria by hemocytes, b: cytoplasm of an epithelial cell showing internalized
372 bacteria, lysosomal body and condensed mitochondria, c: detail of lysosome digesting bacteria, d: fluorescent
373 micrograph showing ORM4-GFP tagged bacteria in close association with gill cell cytoplasm. b: bacteria around cells,
374 ec: epithelial cell, lb: lysosomal body, pl: primary lysosome, sl : secondary lysosome , nu: nucleus, m: mitochondria,
375 ml: lysosomal multilamellar membrane, p: pseudopodia of the phagocytosis vesicle, arrows: internal bacteria.

376

377 **Figure 5.** Effect of the pathogenic strain ORM4 (a) and the non-pathogenic LMG7890 strain (b) of *V. harveyi* on the
378 metabolic activity of gill cells. XTT response from 4-day-old subcultures after 1, 5 and 20 hours of contact with dead
379 bacteria (D), and for ratio of 10, 50 and 100 bacteria/cell. Data are the means \pm SE of six values of two independent
380 experiments. Significant differences ($p < 0.05$) from absorbances measured in control cells are indicated by an asterisk.

381

382 **Figure 6.** Effect of the pathogenic strain ORM4 (a) and the non-pathogenic LMG7890 strain (b) *V. harveyi* on immune

383 response of gill cells, measured by the phenoloxidase activity (PO) after 1, 5 and 18 hours of contact with bacteria
384 killed by boiling (D), and for ratio of 25, 75, 100 and 200 bacteria per cell. Data are the means \pm SE of three values of
385 independent triplicate experiment. Significant differences ($p < 0.05$) from control cells are indicated by an asterisk.

386

387 REFERENCES

388 Alday-Sanz V (2002) Clearing mechanisms on *Vibrio vulnificus* biotype I in the black tiger shrimp *Penaeus monodon*.
389 Dis Aquat Org 48:91-99

390

391 Allam B, Paillard C, Ford SE (2002) Pathogenicity of *Vibrio tapetis*, the etiologic agent of browning disease in clams.
392 Dis Aquat Org 48:221-231

393

394 Allam B, Ford SE (2006) Effects of the pathogenic *Vibrio tapetis* on defence factors of susceptible and non-susceptible
395 bivalve species. 1. Haemocyte changes following *in vitro* challenge. Fish & Shellfish Immunol 20:374-383

396

397 Austin B, Zhang ZH (2006) *Vibrio harveyi*: a significant pathogen of marine vertebrates and invertebrates. Lett Appl
398 Microbiol 43:119-124

399

400 Auzoux-Bordenave S, Domart-Coulon I (2010) Marine Invertebrate cell cultures as tools for biomineralization studies.
401 J Sci Hal Aquat 2:42-47

402

403 Auzoux-Bordenave S, Fouchereau-Peron M, Helleouet M-N, Doumenc D (2007) CGRP regulates the activity of mantle
404 cells and hemocytes in abalone primary cell cultures (*Haliotis tuberculata*). J Shellfish Res 26(3):887-894

405

406 Azevedo C, Balseiro P, Casal G, Gestal C, Aranguren R, Stokes NA, Carnegie RB, Novoa B, Burreson EM Figueras A
407 (2006) Ultrastructural and molecular characterization of *Haplosporidium montforti* n. sp., parasite of the European
408 abalone *Haliotis tuberculata*. J Invertebr Pathol 92 (1):23-32

409

410 Bachère E, Mialhe E, Noël D, Boulo V, Morvan A, Rodriguez J (1995) Knowledge and research prospects in marine
411 mollusc and crustacean immunology. Aquaculture 132:17-32

412

413 Balseiro P, Aranguren R, Gestal C, Novoa B, Figueras A (2006) *Candidatus Xenohaliotis californiensis* and
414 *Haplosporidium montforti* associated with mortalities of abalone *Haliotis tuberculata* cultured in Europe. Aquaculture

415 258:63-72

416

417 Bradford MM (1976) A refined and sensitive method for quantification of microgram quantities of proteins utilizing the
418 principl of protein-dye binding. Anal Biochem 72:248-254

419

420 Boettcher KJ, Barber BJ, Singer JT (1999) Use of antibacterial agents to elucidate the etiology of Juvenile Oyster
421 Disease (JOD) in *Crassostrea virginica* and numerical dominance of an a-proteobacterium in JOD-affected animals.
422 Appl Environ Microbiol 65:2534-2539

423

424 Boettcher KJ, Barber BJ, Singer JT (2000) Additional evidence that juvenile oyster disease is caused by a member of
425 the *Roseobacter* group and colonization of nonaffected animals by *Stappia stellulata*_like strains. Appl Environ
426 Microbiol 66:3924-3930

427

428 Boulo V, Hervio D, Morvan A, Bachere E, Mialhe E (1991) *In vitro* culture of mollusc hemocytes. Functional study of
429 burst respiratory activity and analysis of interactions with protozoan and procaryotic pathogens. In vitro 27:56-64

430

431 Burgents JE, Burnett LE, Stabb EV, Burnett KG (2005) Localization and bacteriostasis of *Vibrio* introduced into the
432 Pacific white shrimp, *Litopenaus vannamei*. Dev Comp Immunol 29:681-691

433

434 Cerenius L, Lee B, Söderhäll K (2008) The proPO-system: pros and cons for its role in invertebrate immunity. Trends
435 Immunol 29:263-271

436

437 Cheng TC (1981) Bivalves: In Ratcliffe NA, Rowley AF (Eds). Invertebrate blood cells. Acadameic Press, London 233-
438 299

439

440 Cheng W, Hsiao IS, Hsu CH, Chen JC (2004a) Change in water temperature on the immune response of Taiwan abalone
441 *Haliotis diversicolor supersexta* and its susceptibility to *Vibrio parahaemolyticus*. Fish Shellfish Immunol 17:235-243

442

443 Cheng W, Juang FM, Chen JC (2004b) The immune response of Taiwan abalone *Haliotis diversicolor supersexta* and
444 its susceptibility to *Vibrio parahaemolyticus* at different salinity levels. Fish Shellfish Immunol 16:295-306

445

446 Coles JA, Pipe RK (1994) Phenoloxidase activity in the hemolymph and hemocytes of the marine mussel *Mytilus*

447 *edulis*. Fish & Shellfish Immunol 4(5):337-352
448
449 Colwell RR (1982) from <http://bccm.belspo.be/about/lmg.php>
450
451 Dang VT, Speck P, Doroudi M, Bekendorff K (2011a) Variation in the antiviral and antibacterial activity of abalone
452 *Haliotis laevis*, *H. rubra* and their hybrid in South Australia. Aquaculture 315:242-249
453
454 Dang VT, Li Y, Speck P, Benkendorff K (2011b) Effects of micro and macroalgal diet supplementations on growth and
455 immunity of greenlip abalone, *Haliotis laevis*. Aquaculture 320:91-98
456
457 De Oliveira David JA, Salaroli RB, Fontanetti CS (2008) Fine structure of *Mytella falcata* (Bivalvia) gill filaments.
458 Micron 39:329-336
459
460 Domart-Coulon I, Auzoux-Bordenave S, Doumenc D, Khalanski M (2000) Cytotoxicity assessment of antibiofouling
461 compounds and by-products in marine bivalve cell cultures. Toxicol in vitro 14(3):245-251
462
463 Faucet J, Maurice E, Gagnaire B, Renault T, Burgeot T (2003). Isolation and primary culture of gill and digestive gland
464 cells from the common mussels *Mytilus edulis*. Methods in Cell Science 23: 177-184.
465
466 Ford SE, Ashton-Alcox SA (1993) *In vitro* interactions between bivalve hemocytes and the oyster pathogen
467 *Haplosporidium nelsoni* (MSX). J Parasitol 79(2):255-265
468
469 Gauger EJ, Gomez-Chiarri M (2002) 16S ribosomal DNA sequencing confirms the synonymy of *Vibrio harveyi* and *V.*
470 *carchariae*. Dis Aquat Organ 52:39-46
471
472 Gaume B, Bourgougnon N, Auzoux-Bordenave S, Roig B, Le Bot B, Bedoux G (2012) *In vitro* effects of triclosan and
473 methyl-triclosan on the marine gastropod *Haliotis tuberculata*. Comp Biochem Physiol C 156(2):87-94
474
475 Handlinger J, Carson J, Donachie L, Gabor L, Taylor D (2005) Bacterial infection in Tasmanian farmed abalone: causes
476 pathology, farm factors and control options. In : Walker P, Lester R, BondadReantaso MG (Eds). Proceedings of the 5th
477 Symposium on Diseases in Asian Aquaculture, Australia, pp 289-300
478

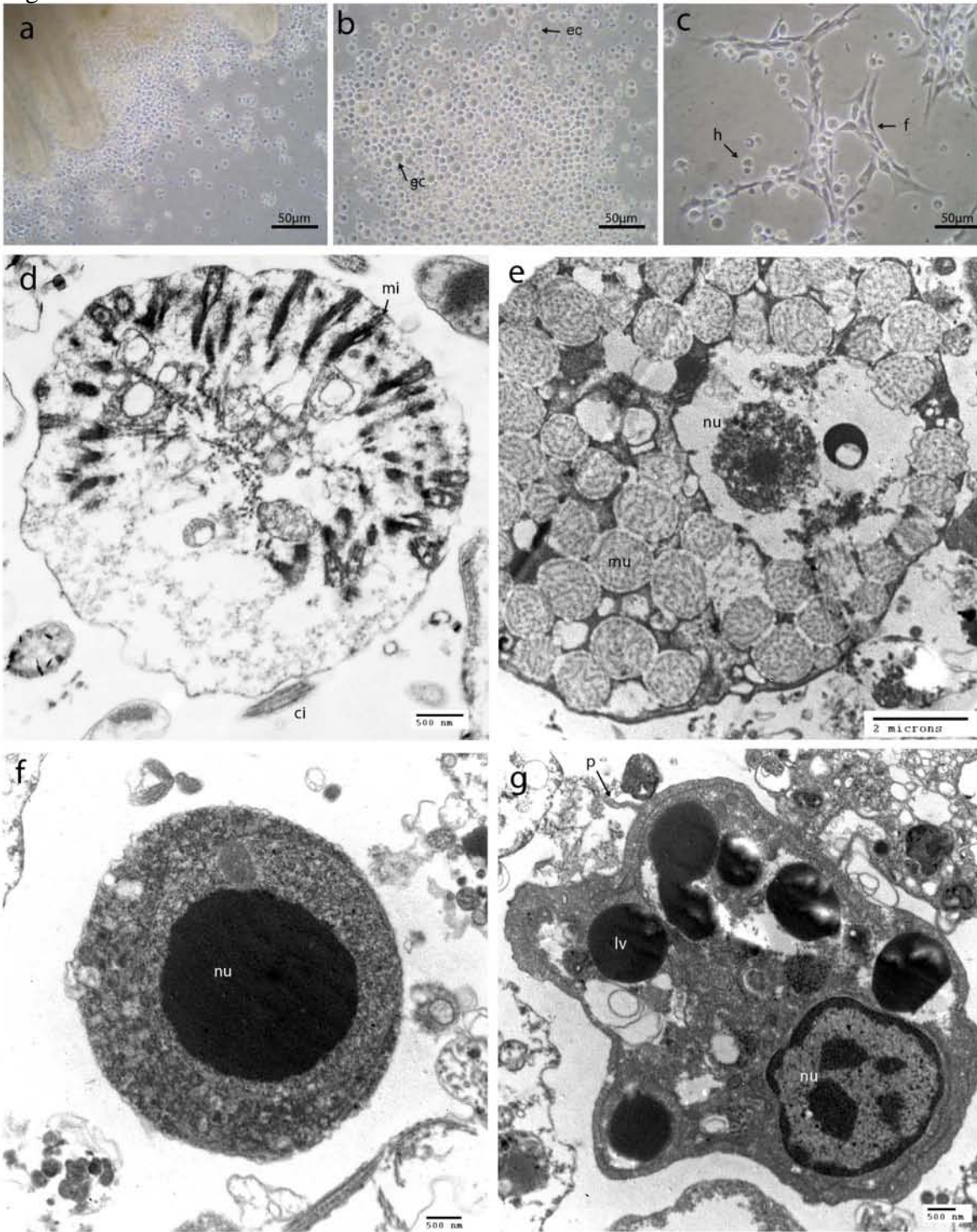
479 Hellio C, Bado-Nilles A, Gagnaire B, Renault T, Thomas-Guyon H (2007) Demonstration of a true phenoloxidase
480 activity and activation of a ProPO cascade in pacific oyster, *Crassostrea gigas* (Thunberg) *in vitro*. Fish Shellfish
481 Immunol 22:433-440
482
483 Hooper C, Day R, Slocombe R, Handlinger J, Benkendorff K (2007) Stress and immune responses in abalone:
484 Limitations in current knowledge and investigative methods based on other models. Fish & Shellfish Immunol
485 22(4):363-379
486
487 Huchette SMH, Clavier J (2004) Status of the ormer (*Haliotis tuberculata* L.) industry in Europe. J Shellfish Res
488 23:951-955
489
490 Kleinschuster SJ, Parent J, Walter CW, Farley CA (1996) A cardiac cell line from *Mya arenaria* (Linnaeus, 1759). J
491 Shellfish Res 15(3):695-707
492
493 Labreuche Y, Soudant P, Goncalves M, Lambert C, Nicolas JL (2006) Effects of extracellular products from the
494 pathogenic *Vibrio aestuarianus* strain 01/32 on lethality and cellular immune responses of the oyster *Crassostrea gigas*.
495 Dev Comp Immunol 30(4):367-379
496
497 Lacoue-Labarthe T, Bustamante P, Horlin E, Luna-Acosta A, Bado-Nilles A, Thomas-Guyon H (2009) Phenoloxidase
498 activation in the embryo of the common cuttlefish *Sepia officinalis* and responses to the Ag and Cu exposure. Fish &
499 Shellfish Immunol 27(3):516-521
500
501 Latire T, Le Pabic C, Mottin E, Mottier A, Costil K, Koueta N, Lebel JM, Serpentine A (2012) Responses of primary
502 cultured haemocytes from the marine gastropod *Haliotis tuberculata* under 10-day exposure to cadmium chloride.
503 Aquatic Toxicol 109:213-221
504
505 Lauckner G (1983) Diseases of Mollusca: Bivalvia. In: Kinne O (Eds) Diseases of Marine Animals Biologische Anstalt
506 Helgoland Hamburg 477-963
507
508 Le Roux F, Gay M, Lambert C, Waechter M, Poubalanne S, Chollet B, Nicolas JLBerthe F (2002) Comparative analysis
509 of *Vibrio splendidus*-related strains isolated during *Crassostrea gigas* mortality events. Aquat Living Resour 15:251-258
510

511 Manganaro M, Laura R, Guerrero MC, Lanteri G, Zaccone D, Marino F (2012) The morphology of gills of *Haliotis*
512 *tuberculata* (Linnaeus, 1758). *Acta Zoologica* 93:436-443
513
514 Martin GG, Poole D, Poole C, Hose JE, Arias M, Reynolds L, McKrell N, Whang A (1993) Clearance of bacteria
515 injected into the haemolymph of the penaeid shrimp, *Syconia ingentis*. *J Invert Pathol* 62:308-315
516
517 Mosmann T (1983) Rapid colorimetric assay for cellular growth and survival: application to proliferation and
518 cytotoxicity assays. *J Immunol Meth* 65:55-63.
519
520 Mottin E, Caplat C, Mahaut ML, Costil K, Barillier D, Lebel JM, Serpentine A (2010) Effect of *in vitro* exposure to zinc
521 on immunological parameters of haemocytes from the marine gastropod *Haliotis tuberculata*. *Fish & Shellfish Immunol*
522 29:846-853
523
524 Nicolas JL, Basuyaux O, Mazurie J, Thebault A (2002) *Vibrio carchariae*, a pathogen of the abalone *Haliotis*
525 *tuberculata*. *Dis Aquat Org* 50:35-43.
526
527 Nishimori E, Hasegawa O, Numata T, Wakabayashi H (1998) *Vibrio carchariae* causes mass mortalities in Japanese
528 abalone, *Sulculus diversicolor supratexta*. *Fish Pathology* 33:495-502
529
530 Paillard C, Maes P (1989) Origine pathogène de l'anneau brun chez *Tapes philippinarum* (Mollusque, bivalve) *C R*
531 *Acad Sci Paris Ser III* 309:235-241
532
533 Paillard C, Leroux F, Borrego JJ (2004) Bacterial diseases in marine bivalves: review of recent studies. *Trends and*
534 *Evol. Aquat Liv Ressour* 17:477-498
535
536 Rinkevich B (1999) Cell cultures from marine invertebrates: obstacles, new approaches and recent improvements. *J*
537 *Biotechnol* 70:133-153
538
539 Rinkevich B (2011) Cell cultures from marine invertebrates: new insights for capturing endless stemness. *Mar*
540 *Biotechnol* 13:345-354
541
542 Rosenberg E, Falkovitz L (2004) The *Vibrio shiloi/Oculina patagonica* model system of coral bleaching. *Annu Rev*

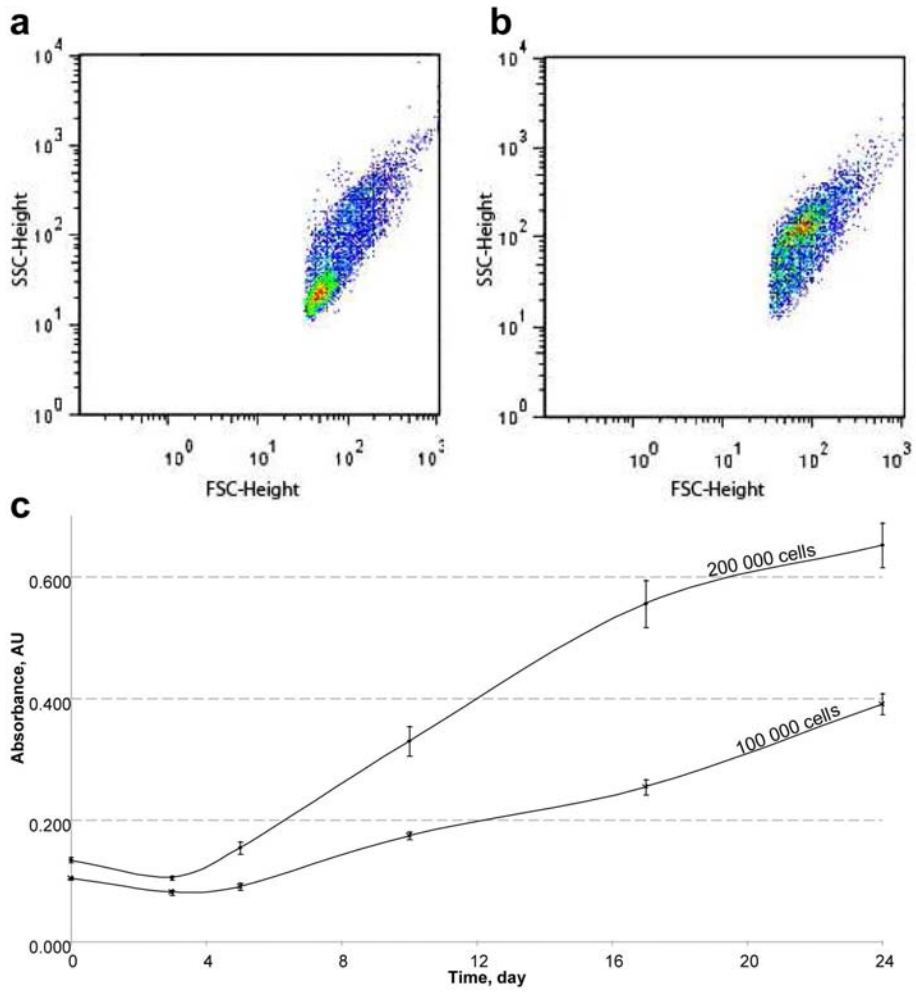
543 Microbiol 58:143-159
544
545 Saulnier D, De Decker S, Haffner P, Cobret L, Robert M, Garcia C (2010) A large-Sscale epidemiological study to
546 identify bacteria pathogenic to pacific oyster *Crassostrea gigas* and correlation between virulence and etalloprotease-
547 like activity. Microb Ecol 59:787-798
548
549 Sharon G, Rosenberg E (2008) Bacterial growth on coral mucus. Current Microbiol 56 :481-488
550
551 Smith VJ (1991) Invertebrate immunology: phylogenetic, ecotoxicological and biomedical implications. Comp
552 Haematol Int 1:60-76
553
554 Suwattana D, Jirasupphachok J, Jarayabhand P, Koykul W (2010) *In vitro* culture of gill and heart tissues of the abalone
555 *Haliotis asinina*. J Shellfish Res 29(3):651-653
556
557 Travers MA, Barbou A, Le Goic N, Huchette S, Paillard C, Koken M (2008a) Construction of a stable GFP-tagged
558 *Vibrio harveyi* strain for bacterial dynamics analysis of abalone infection. FEMS Microbiol Lett 289:34-40
559
560 Travers MA, Le Goic N, Huchette Skoken M, Paillard C (2008b) Summer immune depression associated with increased
561 susceptibility of the European abalone *Haliotis tuberculata* to *Vibrio harveyi* infection. Fish Shellfish Immunol 25:800-
562 808
563
564 Travers MA, Da Silva PM, Le Goic N, Marie D, Donval A, Huchette SMH, Koken M, Paillard C (2008c) Morphologic,
565 cytometric and fonctionnal characterization of abalone (*Haliotis tuberculata*) hemocytes. Fish Shell Immunol 24:400-
566 411
567
568 Travers MA, Le Bouffant R, Friedman CS, Buzin F, Cougard B, Huchette S, Koken M, Paillard C (2009) Pathogenic
569 *Vibrio harveyi*, in contrast to non pathogenic strains, intervenes with the p38 MAPK pathway to avoid an abalone
570 haemocyte immune response. J Cell Biochem 106:152-160
571
572 Vakalia S, Benkendorff K (2005) Antimicrobial activity in the haemolymph of *Haliotis laevigata* and the effects of a
573 dietary immunostimulant. Fleming, A (Ed). The 12th Annual Abalone Aquaculture Workshop. Abalone Aquaculture
574 Subprogram, Fisheries Research and Development Corporation, Canberra, Australia, McLarren Vale, South of Australia

575

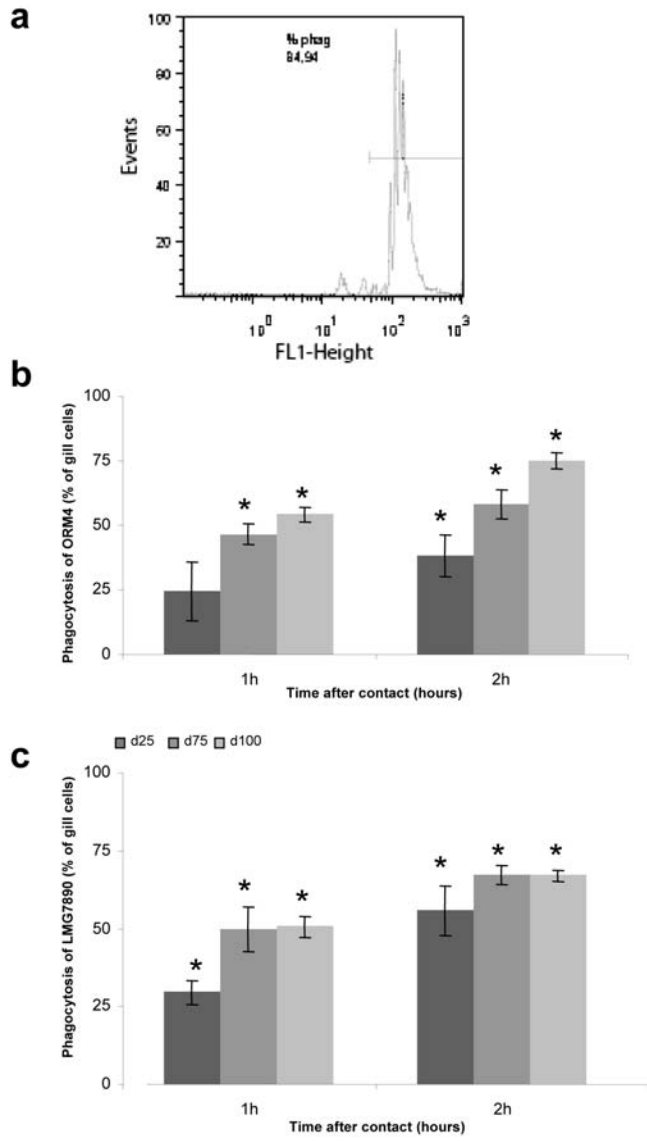
576 Van der Merwe M, Auzoux-Bordenave S, Niesler C, Roodt-Wilding R (2010) Investigating the establishment of
577 primary cell culture from different abalone (*Haliotis midae*) tissues. Cytotechnol 62:265-277



581 Figure 2

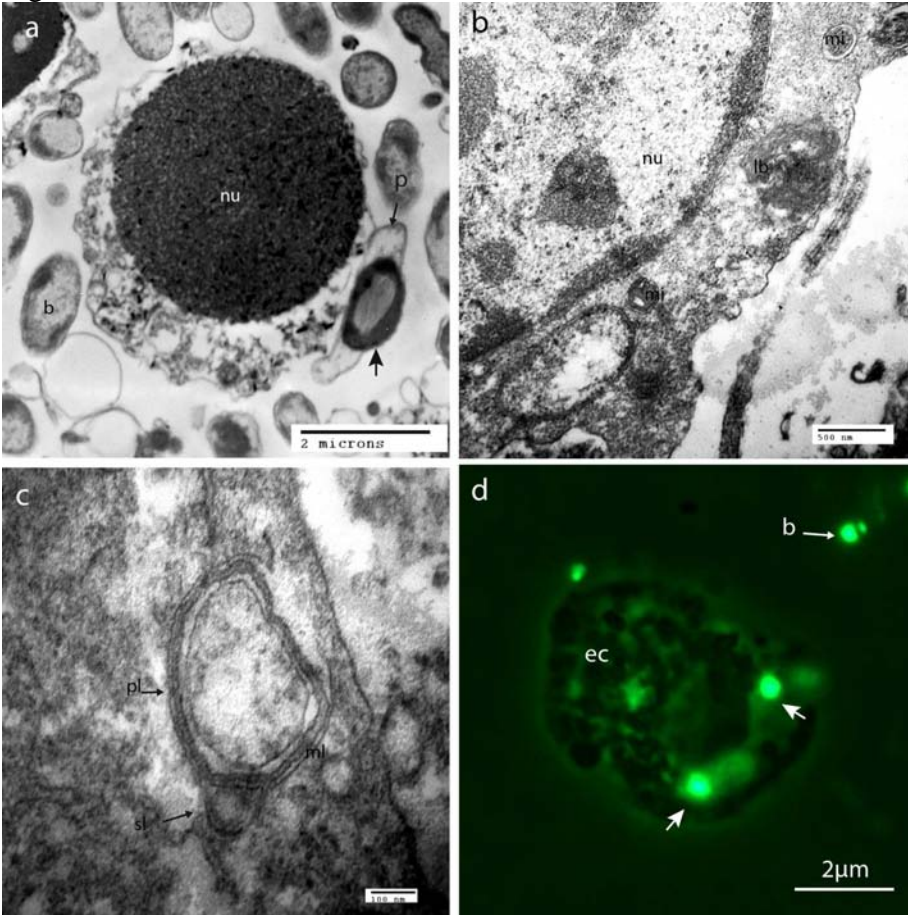


582
583



585
586

587 Figure4



588
589

